nature biomedical engineering

Supplementary information

https://doi.org/10.1038/s41551-024-01242-2

Contributions of network structure, chemoarchitecture and diagnostic categories to transitions between cognitive topographies

In the format provided by the authors and unedited

Contents

Supplementary figures

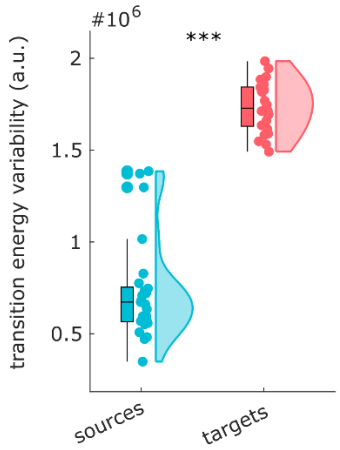

Supplementary Fig. 1 | The 25-term subset reflects asymmetry of transitions. Variability (standard deviation) of transition energy is greater along the column dimension (target states) than along the row dimension (source states), for the reduced set of n=25 brain states reported in Fig.2b; $t(48) = 16.02$, $p < 0.001$, Cohen's $d = 4.46$ from paired-samples t-test (two-sided). Box-plots: center line, median; box limits, upper and lower quartiles; whiskers, 1.5× interquartile range; ***, $p < 0.001$.

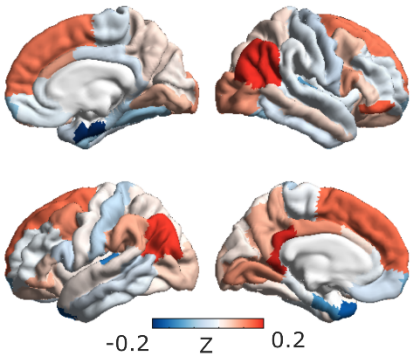

Supplementary Fig. 2 l Cortical topography of high-centrality states in the network of transition energies l Surface projection of the centroid (median) of cortical maps corresponding to cognitive topographies with non-zero betweenness centrality in the network of transitions.

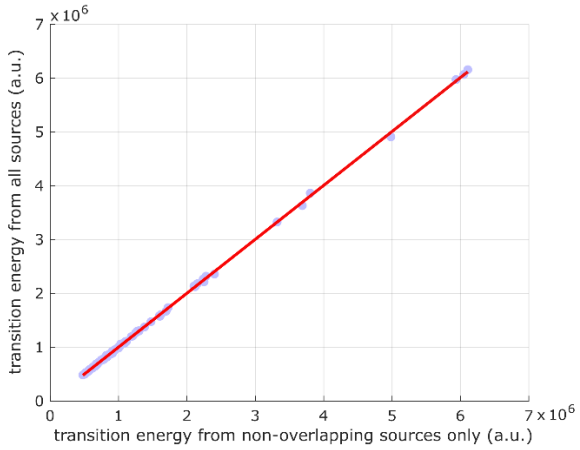

Supplementary Fig. 3 l Removing nested and overlapping NeuroSynth terms does not alter the ranking of cognitive topographies' difficulty to reach. Correlation between transition energy to the cognitive topographies pertaining to non-overlapping terms, from all terms (ordinate), or from non-overlapping terms only (abscissa).

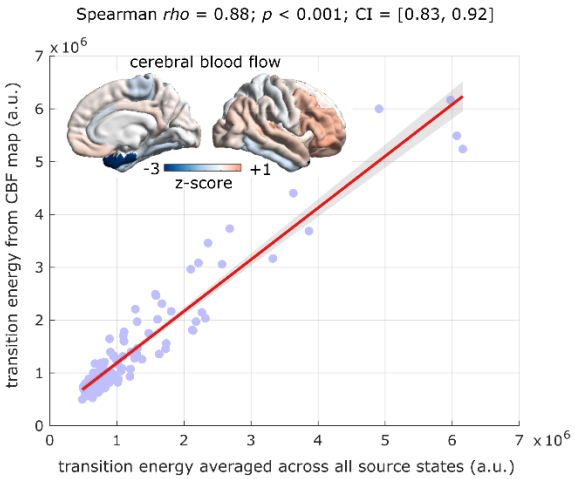

Supplementary Fig. 4 l Transition costs between cognitive topographies recapitulate transition costs from baseline. Spearman correlation (two-sided) between average transition energy starting from n=123 cognitive topographies (abscissa) and starting from a map corresponding to z-scored regional cerebral blood flow (CBF, shown plotted on the cortical surface).

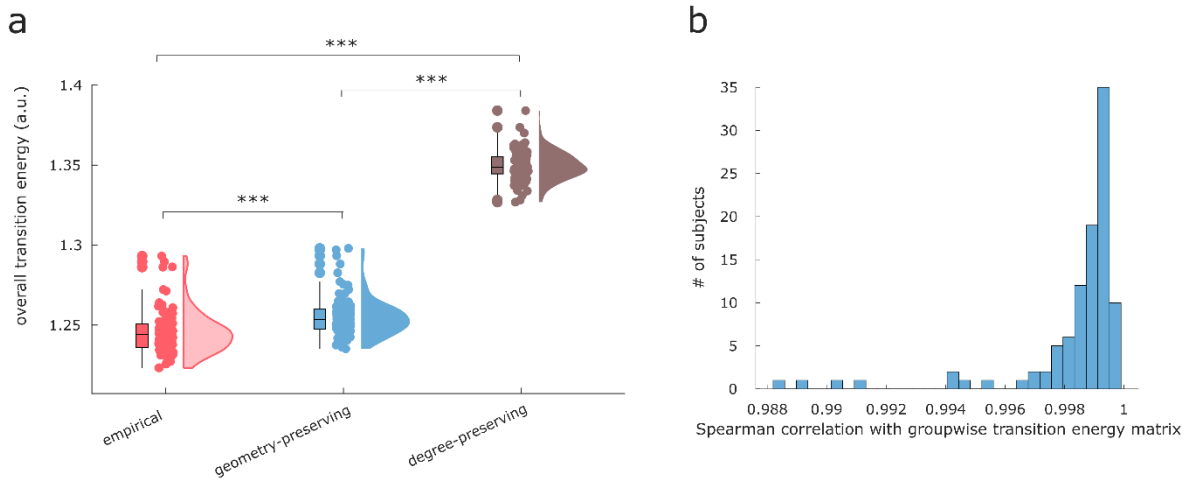

Supplementary Fig. 5 | Replication at the single-participant level. (a) Overall transition energy (averaged across all transitions), for each of n=100 participants and for the corresponding degree- and cost-preserving nulls. Box-plots: center line, median; box limits, upper and lower quartiles; whiskers, 1.5× interquartile range; ***, $p < 0.001$ from paired-samples t-tests (two-sided). **(b)** Histogram of the correlation between each participant's matrix of transition energies, and the matrix of transition energies obtained from the group-wise consensus structural connectome.

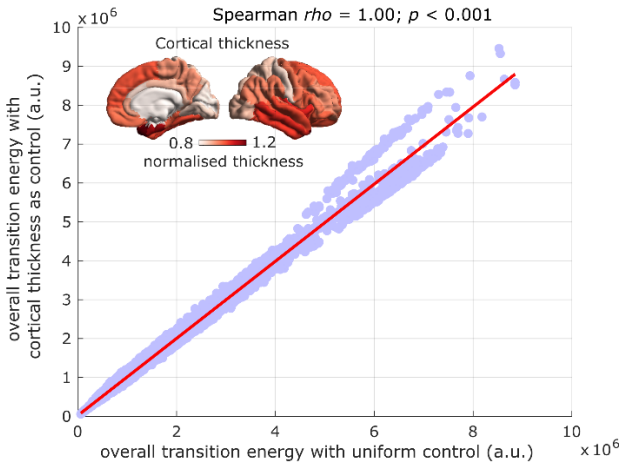

Supplementary Fig. 6 l Transition energy using uniform versus regionally heterogenous control inputs based on regional cortical thickness. Spearman correlation (two-sided) between overall transition energy between all pairs of n=123 cognitive topographies using uniform control inputs at each region (abscissa) and using control inputs proportional to the regional cortical thickness (shown plotted on the surface), scaled to have unit mean (ordinate).

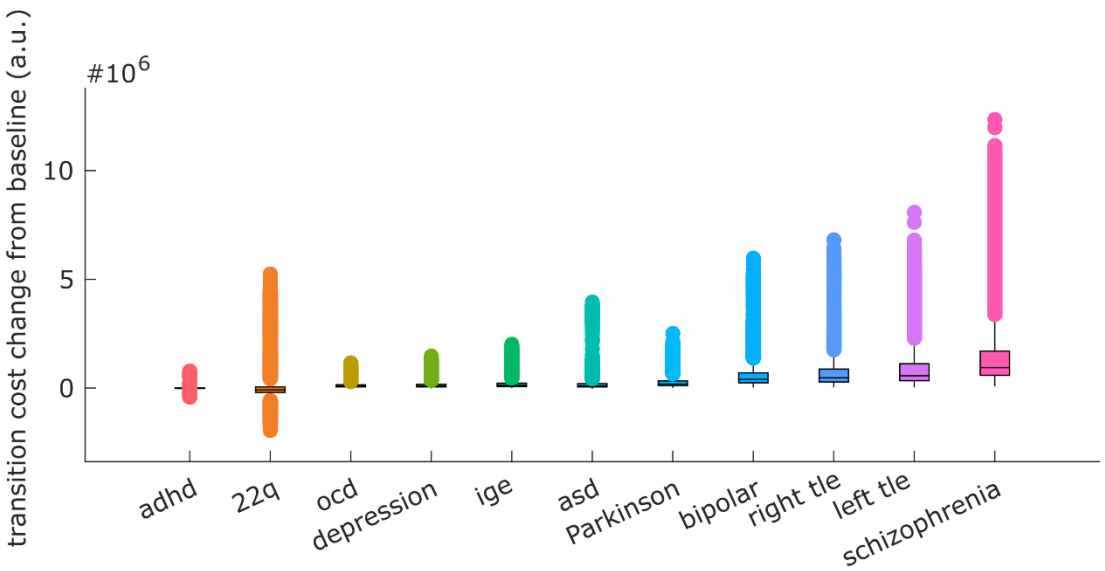

Supplementary Fig. 7 | Overall transition energy when applying control inputs according to maps of cortical thickness change. Each data-point represents the energy to transition to one target state (n=123), averaging across all source states. Boxplots: center line, median; box limits, upper and lower quartiles; whiskers, 1.5× interquartile range; points, outliers.

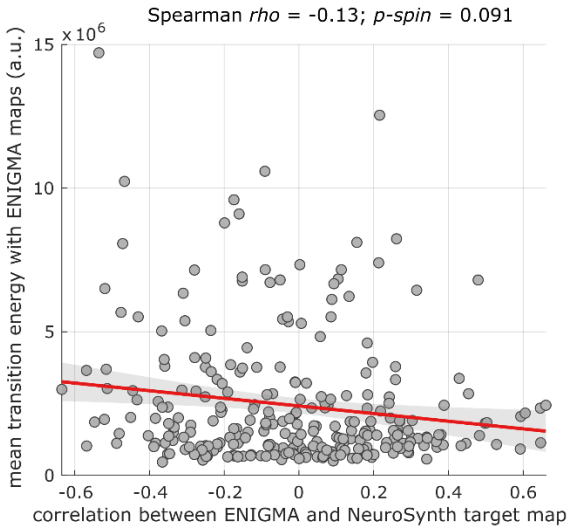

Supplementary Fig. 8 | Spatial correspondence between ENIGMA maps and NeuroSynth maps does not correlate with transition energy. Abscissa: spatial correlation between each ENIGMA map, and the NeuroSynth map associated with each cognitive topography from the subset of 25 used for Fig.4. Ordinate: energy to reach a given cognitive topography in the subset of 25 (averaged across all starting topographies from the same subset) using a given ENIGMA map as input. Correlation between the two distributions is not significant against a null distribution of correlations obtained from 1,000 spatial autocorrelation-preserving rotations of the NeuroSynth maps.

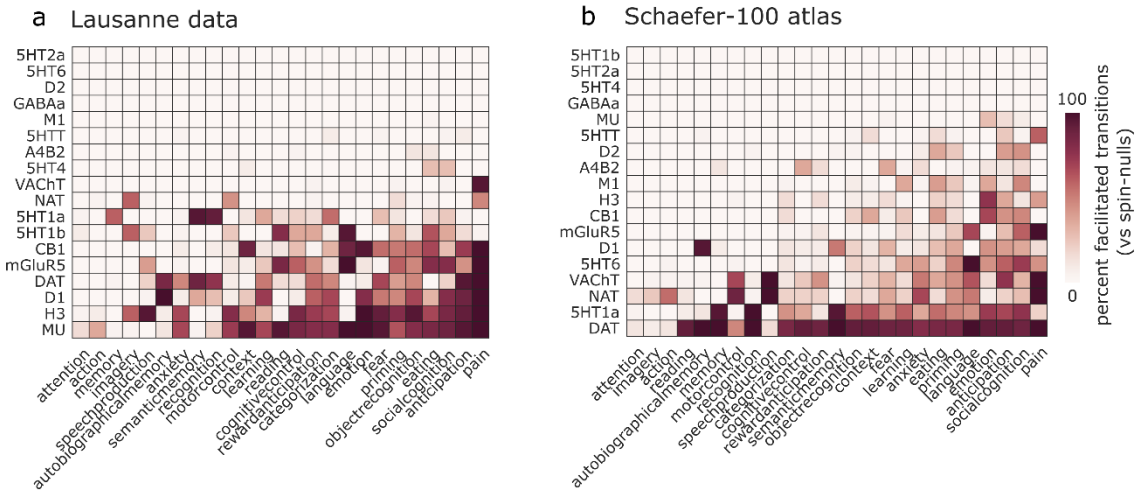

Supplementary Fig. 9 | How neurotransmitter systems can reshape the energy landscape of the human brain, for alternative connectome dataset and alternative cortical parcellation. Heatmaps show how each receptor/transporter reshapes the average cost of reaching a given cognitive brain state from all other states, as a percentage of transitions to each state that are facilitated, when compared against a null distribution of randomly rotated maps with preserved spatial autocorrelation and the same receptor/transporter density levels, but occurring at different neuroanatomical locations. **(a)** For the Lausanne DSI dataset; **(b)** for Human Connectome Project data parcellated using the Schaefer-100 cortical atlas.

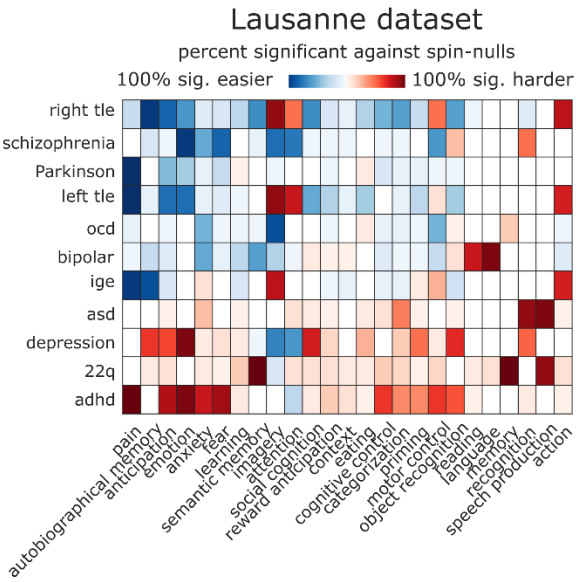

Supplementary Fig. 10 l Effects of cortical thickness changes associated with each diagnostic category, for alternative connectome dataset and alternative cortical parcellation. Heatmap shows how each diagnostic category reshapes the transition energy required to reach a given cognitive topography, presented as the percentage of transitions (out of all possible initial cognitive topographies) that are significantly facilitated (blue colour scale) or significantly dis-facilitated (red colour scale). Significance is assessed against a null distribution of randomly rotated cortical thickness alteration maps with preserved mean, variance, and spatial autocorrelation, such that the only differences with the original map are the neuroanatomical locations of increases and decreases, for the Lausanne DSI dataset. adhd = attention deficit/hyperactivity disorder; asd = autistic spectrum disorder; ocd = obsessive-compulsive disorder; ige = idiopathic generalised epilepsy; right tle = right temporal lobe epilepsy; left tle = left temporal lobe epilepsy.

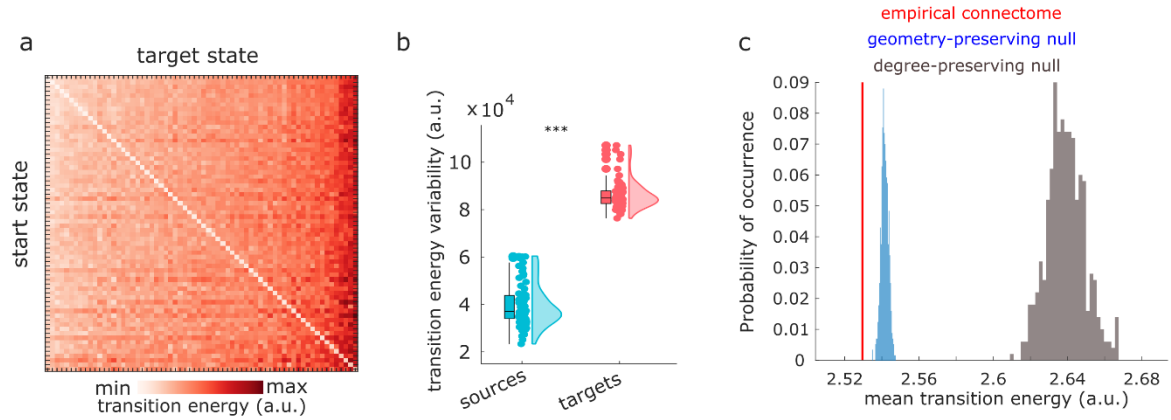

Supplementary Fig. 11 | Replication with cognitive topographies defined by BrainMap. a Transition energy between each pair of n = 66 cognitive topographies from BrainMap. **b** Variability (standard deviation) of transition energy is greater along target states than along start states (n=66). Box-plots: center line, median; box limits, upper and lower quartiles; whiskers, 1.5×interquartile range; ***, $p < 0.001$ from independent-samples t-tests (two-sided). **c** Degree-preserving randomised null models (grey) and null models that preserve the exact degree sequence and the approximate length distribution (blue) are significantly less favourable than the empirical human connectome (red) to support transitions between cognitive topographies defined by BrainMap.

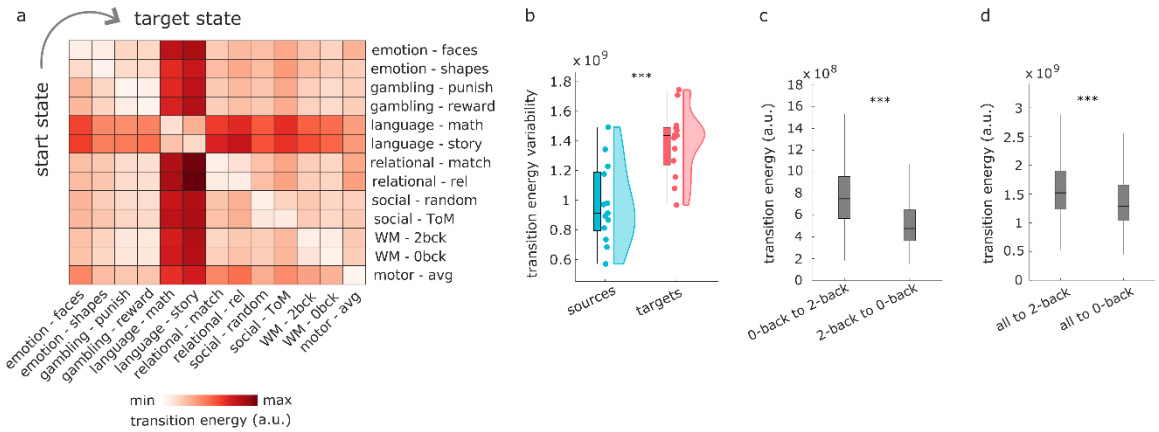

Supplementary Fig. 12 | Transition energy between individual-level cognitive topographies defined from in-scanner task contrasts. a Transition cost (energy) between each pair of 13 cognitive topographies defined as individual-specific task contrasts from 7 different tasks, across n=989 HCP participants. Rows indicate source states, columns indicate target states. **b** Variability (standard deviation) of transition energy is greater along the column dimension (target states, n=13) than along the row dimension (source states, n=13); $t(24) = 4.24$, $p < 0.001$, Cohen's $d = 1.61$. Box-plots: center line, median; box limits, upper and lower quartiles; whiskers, 1.5× interquartile range; ***, $p < 0.001$ from independent-samples t-tests (two-sided). **c** Transition cost (energy) is greater when transitioning from the subjectively easier 0-back working memory task to the subjectively more demanding 2-back working memory task, than the reverse ($t(985) = 20.58$, $p < 0.001$, Cohen's $d = 0.50$, n=986 participants). Box-plots: center line, median; box limits, upper and lower quartiles; whiskers, 1.5× interquartile range; ***, $p < 0.001$ from paired-samples t-tests (two-sided). **d** Transition cost (energy) is greater when transitioning from any task to the demanding 2-back working memory task, than from any task to the easier 0-back task ($t(951) = 13.16$, $p < 0.001$, Cohen's $d = 0.26$, n=952 participants). Box-plots: center line, median; box limits, upper and lower quartiles; whiskers, 1.5× interquartile range; ***, $p < 0.001$ from paired-samples t-tests (two-sided).

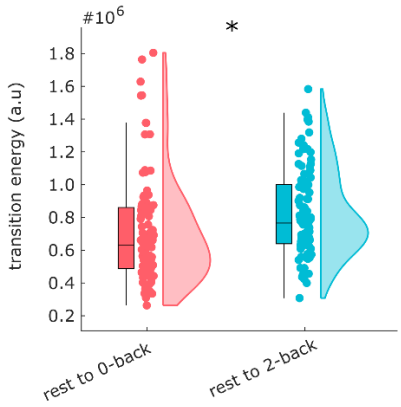

Supplementary Fig. 13 | Energy for empirical transitions between temporally adjacent blocks during the working memory scan. We computed the energy corresponding to each transition between temporally adjacent rest and task blocks, for each of the n=100 unrelated individuals in the HCP dataset. On average, transitions from rest blocks to subsequent 0-back blocks require less energy than transitions from rest blocks to subsequent 2-back blocks ($t(99) = 2.52$, $p = 0.013$, Cohen's $d = 0.39$). Box-plots: center line, median; box limits, upper and lower quartiles; whiskers, 1.5× interquartile range; ***, $p < 0.05$ from paired-samples t-test (two-sided).

Supplementary tables

Supplementary Table 1 | Participant-level comparison against null networks. Statistical comparison (from paired-samples t-tests, two-sided) between participant-level overall transition energy distributions, for the empirical human connectome (n = 100 Human Connectome Project participants) and corresponding degree-preserving and degree- and cost-preserving rewired nulls.

	Mean1	SD1	Mean2	SD2	df	t-score	p-value	Effect Size
empirical vs geometry-preserving	1.25e+06	13400	1.26e+06	12200	99	-21.49	<0.001	-0.77
empirical vs degree-preserving	1.25e+06	13400	1.35e+06	9160	99	-60.18	<0.001	-9.05
degree- vs geometry-preserving	1.35e+06	9160	1.26e+06	12200	99	58.92	<0.001	8.7

Supplementary Table 2 | Participant-level results for alternative implementation of network control theory. Statistical comparison (from paired-samples t-tests, two-sided) between participant-level overall transition energy distributions, for the empirical human connectome (n = 100 HCP participants) and corresponding degree-preserving and degree- and cost-preserving rewired nulls, for network control with time horizon T = 3 and network normalisation factor $c = 0.01 \times |\lambda(A)_{max}|$.

	Mean1	SD1	Mean2	SD2	df	t-score	p-value	Effect Size
empirical vs geometry-preserving	1.27e+06	9560	1.28e+06	9630	69	-15.03	<0.001	-1.1
empirical vs degree-preserving	1.27e+06	9560	1.35e+06	11300	69	-44.91	<0.001	-7.3
degree- vs geometry-preserving	1.35e+06	11300	1.28e+06	9630	69	36.34	<0.001	6.3

Supplementary Table 3 | Participant-level results for alternative implementation of network control theory. Statistical comparison (from paired-samples t-tests, two-sided) between participant-level overall transition energy distributions, for the empirical human connectome (n = 100 HCP participants) and corresponding degree-preserving and degree- and geometry-preserving rewired nulls, for network control with NeuroSynth maps normalised to unit Euclidean norm.

	Mean1	SD1	Mean2	SD2	df	t-score	p-value	Effect Size
empirical vs geometry-preserving	1.3e+06	17200	1.31e+06	14900	99	-17.38	<0.001	-0.76
empirical vs degree-preserving	1.3e+06	17200	1.42e+06	8480	99	-64.11	<0.001	-8.6
degree- vs geometry-preserving	1.42e+06	8480	1.31e+06	14900	99	65.11	<0.001	8.7

Supplementary Table 4 | Participant-level results for the Lausanne dataset. Statistical comparison (from paired-samples t-tests, two-sided) between participant-level overall transition energy distributions, for the empirical human connectome (n = 70 participants from the Lausanne dataset) and corresponding degree-preserving and degree- and cost-preserving rewired nulls.

	Mean1	SD1	Mean2	SD2	df	t-score	p-value	Effect Size
empirical vs geometry-preserving	3.03e+05	7640	2.99e+05	7460	99	14.81	<0.001	0.49
empirical vs degree-preserving	3.03e+05	7640	2.65e+05	4140	99	50.37	<0.001	6.1
degree- vs geometry-preserving	2.65e+05	4140	2.99e+05	7460	99	-47.26	<0.001	-5.6

Supplementary Table 5 | Participant-level results for Schaefer-parcellated data. Statistical comparison (from paired-samples t-tests, two-sided) between participant-level overall transition energy distributions, for the empirical human connectome (n = 100 participants from the Human Connectome Project) and corresponding degree-preserving and degree- and cost-preserving rewired nulls.

	Mean1	SD1	Mean2	SD2	df	t-score	p-value	Effect Size
empirical vs geometry-preserving	35500	312	35800	298	99	-27.19	<0.001	-0.84
empirical vs degree-preserving	35500	312	38100	260	99	-61.91	<0.001	-9.02
degree- vs geometry-preserving	38100	260	35800	298	99	58.64	<0.001	8.3

Supplementary Table 6 | NeuroSynth terms. Terms that overlapped between the NeuroSynth database [8] and the Cognitive Atlas [62] were included in the analysis.

action	adaptation	addiction	anticipation	anxiety
arousal	association	attention	autobiographical memory	balance
belief	categorization	cognitive control	communication	competition
concept	consciousness	consolidation	context	coordination
decision	decision making	detection	discrimination	distraction
eating	efficiency	effort	emotion	emotion regulation
empathy	encoding	episodic memory	expectancy	expertise
extinction	face recognition	facial expression	familiarity	fear
fixation	focus	gaze	goal	hyperactivity
imagery	impulsivity	induction	inference	inhibition
insight	integration	intelligence	intention	interference
judgment	knowledge	language	language comprehension	learning
listening	localization	loss	maintenance	manipulation
meaning	memory	memory retrieval	mental imagery	monitoring
mood	morphology	motor control	movement	multisensory
naming	navigation	object recognition	pain	perception
planning	priming	psychosis	reading	reasoning
recall	recognition	rehearsal	reinforcement learning	response inhibition
response selection	retention	retrieval	reward anticipation	rhythm
risk	rule	salience	search	selective attention
semantic memory	sentence comprehension	skill	sleep	social cognition
spatial attention	speech perception	speech production	strategy	strength
stress	sustained attention	task difficulty	thought	uncertainty
updating	utility	valence	verbal fluency	visual attention
visual perception	word recognition	working memory		

Supplementary Table 7 | Nested terms. Nested terms are more specific versions of the superordinate ones. Additionally, overlapping but not nested terms are also present, such as “sentence comprehension” and “language comprehension”, “speech perception” and “speech production”, or “face recognition” and “facial expression”; “cognitive control” and “motor control”.

Superordinate term	Nested terms
Anticipation	reward anticipation
Attention	selective attention
	spatial attention
	sustained attention
	visual attention
Decision	decision making
Emotion	emotion regulation
Imagery	mental imagery
Language	language comprehension
Learning	reinforcement learning
Memory	working memory
	autobiographical memory
	episodic memory
	memory retrieval
	semantic memory
Recognition	facial recognition
	object recognition
	word recognition
Response	response inhibition
	response selection
Perception	visual perception

Supplementary Table 8 | BrainMap terms. BrainMap terms are organized by behavioural domain. All 66 unique behavioural domain (excluding any undefined domains) used in analyses are shown here.

air-hunger	disgust	language	phonology	speech (action)
alcohol	emotion	learning	preparation	speech (language)
amphetamines	estrogen	marijuana	psychiatric medications	SSRIs
anger	execution	memory	reasoning	steroids and hormones
antidepressants	explicit	motion	rest	syntax
antipsychotics	fear	music	sadness	thermoregulation
anxiety	gustation	nicotine	semantics	thirst
attention	happiness	non-steroidal anti-inflammatory drugs	sexuality	time
audition	humour	observation	shape	vision
bladder	hunger	olfaction	sleep	working memory
caffeine	imagination	opioids	social cognition	
capsaicin	inhibition	orthography	soma	
cognition	interoception	pain	somesthesis	
colour	ketamine	pharmacology	space	